

HNPS Advances in Nuclear Physics

Vol 20 (2012)

HNPS2012



Differential cross-section measurements for the $7\text{Li}(p,p_0)7\text{Li}$, $7\text{Li}(p,p_1)7\text{Li}$, $7\text{Li}(p,\alpha_0)4\text{He}$, $^{19}\text{F}(p,p_0)^{19}\text{F}$, $^{19}\text{F}(p,\alpha_0)^{16}\text{O}$ and $^{19}\text{F}(p,\alpha_1,2)^{16}\text{O}$ reactions

V. Paneta, A. Lagoyannis, A. Kafkarkou, M. Kokkoris

doi: [10.12681/hnps.2492](https://doi.org/10.12681/hnps.2492)

To cite this article:

Paneta, V., Lagoyannis, A., Kafkarkou, A., & Kokkoris, M. (2012). Differential cross-section measurements for the $7\text{Li}(p,p_0)7\text{Li}$, $7\text{Li}(p,p_1)7\text{Li}$, $7\text{Li}(p,\alpha_0)4\text{He}$, $^{19}\text{F}(p,p_0)^{19}\text{F}$, $^{19}\text{F}(p,\alpha_0)^{16}\text{O}$ and $^{19}\text{F}(p,\alpha_1,2)^{16}\text{O}$ reactions. *HNPS Advances in Nuclear Physics*, 20, 89–95. <https://doi.org/10.12681/hnps.2492>

Differential cross-section measurements for the ${}^7\text{Li}(\text{p},\text{p}_0){}^7\text{Li}$, ${}^7\text{Li}(\text{p},\text{p}_1){}^7\text{Li}$, ${}^7\text{Li}(\text{p},\alpha_0){}^4\text{He}$, ${}^{19}\text{F}(\text{p},\text{p}_0){}^{19}\text{F}$, ${}^{19}\text{F}(\text{p},\alpha_0){}^{16}\text{O}$ and ${}^{19}\text{F}(\text{p},\alpha_{1,2}){}^{16}\text{O}$ reactions

V. Paneta^a, A. Lagoyannis^a, A. Kafkarkou^b, M. Kokkoris^b

^a*Tandem Accelerator Laboratory, Institute of Nuclear Physics, N.C.S.R.*

“Demokritos”, Aghia Paraskevi, 15310 Athens, Greece

^b*Department of Physics, National Technical University of Athens, Zografou campus, 15780 Athens, Greece*

Abstract

Differential cross sections of the ${}^7\text{Li}(\text{p},\text{p}_0){}^7\text{Li}$, ${}^7\text{Li}(\text{p},\text{p}_1){}^7\text{Li}$, ${}^7\text{Li}(\text{p},\alpha_0){}^4\text{He}$, ${}^{19}\text{F}(\text{p},\text{p}_0)$, ${}^{19}\text{F}(\text{p},\alpha_0){}^{16}\text{O}$ and ${}^{19}\text{F}(\text{p},\alpha_{1,2}){}^{16}\text{O}$ reactions have been determined for proton energies $E_{\text{lab}}=1500\text{-}7000$ keV, using a variable energy step and for detection angles between 140° - 170° in steps of 10° . To validate the obtained results, benchmarking measurements were performed, using thick and mirror-polished BaF_2 and LiF targets. The experimental data are compared to data from literature, when available, and similarities and discrepancies are presented and analyzed.

1 Introduction

Lithium and fluorine are very common elements in nature with a huge technological interest. The main problem concerning the depth profiling of lithium and fluorine is that since both elements are highly reactive, they are usually present in relatively complex matrices along with several medium- or high-Z elements. Thus, the determination of their profile concentrations presents strong analytical challenges for all IBA techniques. Among these techniques, Elastic Backscattering Spectroscopy (EBS –denoting deviations from the Rutherford formula) and Nuclear Reaction Analysis (NRA) are preferably used, due to their high analytical power for accurate and simultaneous determination of several light element concentrations in complex samples.

The existing differential cross-section datasets in the literature, necessary for the implementation of these techniques, are unfortunately inadequate and dis-

crepant in many cases, thus limiting the applicability of both methods. More specifically, for the study of lithium concentration depth profiles, ${}^7\text{Li}({}^3\text{He},\alpha_0){}^6\text{Li}$, ${}^7\text{Li}({}^3\text{He},d){}^8\text{Be}$, ${}^7\text{Li}({}^3\text{He},p){}^9\text{Be}$, ${}^7\text{Li}(p,p_0){}^7\text{Li}$ and ${}^7\text{Li}(p,\alpha_0){}^4\text{He}$ reactions have been proposed in the past [1-8]. The most promising one though, seems to be the ${}^7\text{Li}(p,\alpha_0){}^4\text{He}$ reaction, because of its relatively high cross-section values and high Q-value, providing isolated peaks with practically no background. There is however a lack of corresponding data in literature over a wide range of energies and detector angles. The present study aims at contributing in this field through the differential cross-section measurements of the ${}^7\text{Li}(p,p_0){}^7\text{Li}$, ${}^7\text{Li}(p,p_1){}^7\text{Li}$, and ${}^7\text{Li}(p,\alpha_0){}^4\text{He}$ reactions, in the energy range of 1.5-7 MeV using a variable energy step and for detection angles between 140° and 170° in steps of 10° .

As far as fluorine is concerned, Proton Induced Gamma-ray Emission (PIGE) is mainly used for the determination of its profile concentrations, due to the existence of several, narrow and strong resonances in the $p+{}^{19}\text{F}$ system (e.g. the relatively narrow, $\Gamma=4.5$ keV resonance at $E_p=872.11$ keV of the ${}^{19}\text{F}(p,\alpha\gamma){}^{16}\text{O}$ reaction). Alternatively, ${}^{19}\text{F}(d,\alpha_0){}^{17}\text{O}$, ${}^{19}\text{F}(d,p_0){}^{20}\text{F}$, ${}^{19}\text{F}(d,p_1){}^{20}\text{F}$, ${}^{19}\text{F}(p,p_0){}^{19}\text{F}$, and ${}^{19}\text{F}(p,\alpha_0){}^{16}\text{O}$ reactions have been proposed in the past. However, several differential cross-section datasets in literature concerning various $p+{}^{19}\text{F}$ reaction channels are discrepant in many cases, mainly because of the complicated resonance structures involved. There has also been a tentative evaluation for proton elastic backscattering from ${}^{19}\text{F}$ for a limited energy range (550-1750 keV) using SigmaCalc [9]. These evaluated differential cross sections are available to the scientific community through the IBANDL nuclear database from IAEA [www-nds.iaea.org/ibandl/].

It is important to note here, that the present work aimed mainly at studying the $p+{}^7\text{Li}$ system. Due to the implemented LiF target though, selected differential cross-section values have also been determined for the ${}^{19}\text{F}(p,p_0){}^{19}\text{F}$, ${}^{19}\text{F}(p,\alpha_0){}^{16}\text{O}$ and ${}^{19}\text{F}(p,\alpha_{1,2}){}^{16}\text{O}$ reactions. It has to be pointed out however, that the adopted energy step was inadequate for a complete study of the strong and narrow resonances existing in the $p+{}^{19}\text{F}$ system. Nevertheless, the determined, coherent differential cross-section datasets from the present work may prove to be valuable for further evaluation purposes.

2 Experimental setup and procedure

The measurements were performed using the proton beam of the 5.5 MV TN11 Tandem Accelerator of N.C.S.R. “Demokritos”, Athens, Greece. Protons were accelerated to $E_{p,lab}=1500-7000$ keV in steps of 100 keV and 25 keV (when close to strong resonances) and were led to a cylindrical scattering chamber of large dimensions ($R\sim 30$ cm). The energy of the protons entering the scat-

tering chamber was determined by nuclear magnetic resonance measurements (NMR) with an estimated ripple of $\sim 0.12\text{--}0.16\%$, as verified by the 991.89 keV resonance of the $^{27}\text{Al}(p,\gamma)^{28}\text{Si}$ reaction at the beginning and at the end of the experiment, using a HPGe detector (of 80% relative efficiency).

The detection system consisted of four Si surface barrier detectors (thickness of 1000 μm) placed at 140° , 150° , 160° and 170° along with the corresponding electronics. The spectra from the four detectors, which were placed at a distance of ~ 9 cm from the target, were simultaneously recorded for each energy interval. Orthogonal slits ($\sim 4.5 \times 8\text{mm}^2$) and small cylindrical tubes, $\sim 7\text{cm}$ long, with a diameter of $\sim 0.3\text{cm}$, were placed in front of the detectors in order to reduce the angular uncertainty to $\sim \pm 1^\circ$ and to impede the detection of scattered protons from the faraday cup and from the chamber walls respectively.

The target for the cross-section measurements consisted of a thin carbon foil of $52 \pm 2 \mu\text{g}/\text{cm}^2$ thickness, with a LiF layer of $(960 \pm 38) \times 10^{15} \text{ at}/\text{cm}^2$ that was evaporated onto the carbon foil and additionally with a thin gold layer of $4.4 \pm 0.3 \mu\text{g}/\text{cm}^2$ that was evaporated onto the LiF layer for protection against wear and humidity absorption. The thickness of the LiF layer was estimated using the evaluated differential cross sections from SigmaCalc calculations [9] for proton elastic scattering on ^{19}F at 160° . Prior to the determination of the LiF thickness in such a way, a benchmarking experiment at 1600 keV was performed for the verification of the evaluated differential cross sections to be used. For this experiment a thick CaF_2 pellet and the SIMNRA code [10] for the simulation of this measurement were used. The simulated spectrum was produced using the evaluated differential cross-section dataset from SigmaCalc for the $^{19}\text{F}(p,p_0)^{19}\text{F}$ scattering, taking into account a very small energy step for the incoming and outgoing protons, the effect of multiple scattering, the beam ripple, Ziegler–Biersack–Littmark [11] stopping power data, and Chu and Yang’s straggling model, as implemented in the SIMNRA code. The elastic scattering on ^{12}C and ^{16}O (on the surface of the pellet) were also simulated using the corresponding evaluated data from SigmaCalc. The spectrum acquired by the detector at 160° could be reproduced by the simulation, only with the evaluated cross sections being increased by 17%. Using these corrected data, the thickness of the fluorine layer in the target was then determined with an accuracy of $\sim 4\%$. The Li:F ratio of the target was measured using transmission ERDA with 5.9 MeV ^{12}C ions and was found to closely approximate 1:1. In order to calculate the mean proton beam energy, the energy loss and the energy straggling in the target in all cases, Monte–Carlo simulations were performed using the computer code SRIM 2010 [12]. Peak fitting/integration yielded an uncertainty not greater than 4% in the integral of the backscattered particles in most cases. A typical experimental spectrum taken at 140° and $E_{p,\text{lab}}=3700$ keV is presented in Fig. 1, along with the corresponding peak identification.

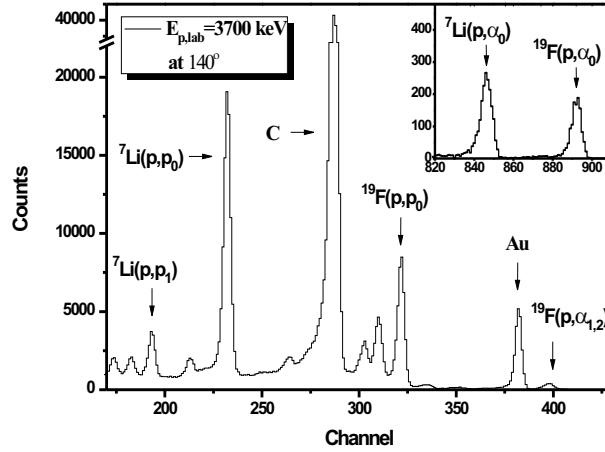


Fig. 1. Typical experimental spectrum taken at 140° and for $E_{p,lab} = 3700 \text{ keV}$, along with the corresponding peak identification.

For the validation of the obtained differential cross sections, benchmarking experiments were performed, using thick, commercial and mirror-polished BaF_2 and LiF targets. For beam normalization purposes Au was evaporated onto the LiF thick target.

3 Data analysis and Results

The determination of the differential cross-section values for ${}^7\text{Li}$ and ${}^{19}\text{F}$ reactions respectively, was carried out following the formulas for relative measurements, compared to the differential cross section of the ${}^{197}\text{Au}(p,p_0)$ reaction, which does not deviate from the Rutherford formula over the whole proton beam energy range, for the same scattering angle and accumulated charge.

Due to the kinematics of all reactions, all peaks in the spectra were isolated over the whole energy range studied, except for a very few cases, e.g. peaks that correspond to ${}^7\text{Li}(p,\alpha_0){}^4\text{He}$ and ${}^{19}\text{F}(p,\alpha_0){}^{16}\text{O}$ reactions coincide for the proton energy range $\sim 2550\text{--}2750 \text{ keV}$ at 150° , thus rendering their independent analysis impossible. The combined statistical errors for the differential cross sections, varying between $\sim 1\text{--}4\%$ for elastic scattering and $\sim 4\text{--}7\%$ for (p,α) reactions, included the uncertainties in peak integration (including counting statistics and background subtraction), while the overall target thickness' uncertainty was $\sim 4\%$. The total experimental uncertainty was calculated following standard error propagation formulas. The reported proton energy values in the laboratory reference frame correspond to the half of the LiF layer's thickness, following SRIM 2010 calculations [12], after the proper correction

according to the results of the accelerator calibration presented in the previous section, with an accuracy of 4-10 keV over the whole studied energy range.

Differential cross-section values obtained in the present study for ${}^7\text{Li}(p,p_0){}^7\text{Li}$, ${}^7\text{Li}(p,\alpha_0){}^4\text{He}$ and ${}^7\text{Li}(p,p_1){}^7\text{Li}$ are presented in detail in IBANDL, along with the corresponding uncertainty (excluding the uncertainty in the determination of the target's thickness). An example is shown here in Fig. 2, along with data from literature [1-8], when available. The error bars shown in the graph for the obtained data are only the statistical experimental errors (excluding the uncertainty in the determination of the target's thickness), while the error bars along the x- axis (energy ripple of 0.16%) are not visible due to the adopted scale.

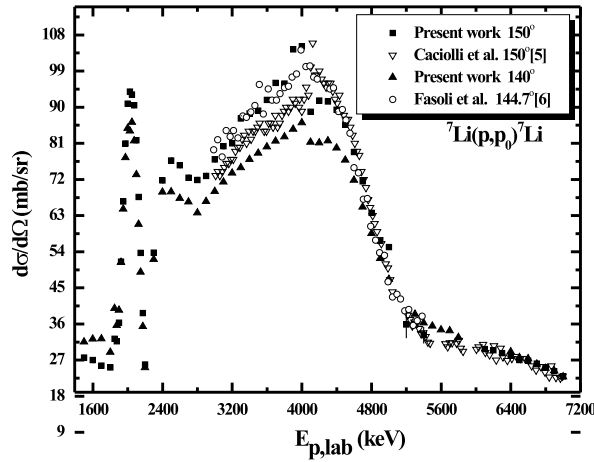


Fig. 2. Differential cross section values (mb/sr) for the ${}^7\text{Li}(p,p_0){}^7\text{Li}$ reaction at 150° , for $E_{p,lab}=1500-7000$ keV along with data from literature, when available

Differential cross sections obtained in the present study for the ${}^{19}\text{F}(p,p_0){}^{19}\text{F}$, ${}^{19}\text{F}(p,\alpha_0){}^{16}\text{O}$ and ${}^{19}\text{F}(p,\alpha_{1,2}){}^{16}\text{O}$ reactions, for the same laboratory detection angles 140° , 150° , 160° and 170° , have also been determined. The alpha groups α_1 , and α_2 , belonging to the 6049 keV and 6130 keV excitation levels of the ${}^{16}\text{O}$ nucleus respectively, could not be analyzed separately, because of the coincidence of the corresponding peaks in the spectra for the proton energy range studied (due to the kinematics).

Due to the observed discrepancies among differential cross-section datasets from literature, a benchmarking procedure using thick targets is critical in order to validate the obtained values. More specifically, benchmarking measurements were performed, using thick and mirror-polished BaF_2 and LiF targets to validate the obtained differential cross sections of the (p,α_0) reactions for both elements (${}^7\text{Li}$ and ${}^{19}\text{F}$) using the SIMNRA code. The simulated spectra were produced using the obtained differential cross-section datasets and taking

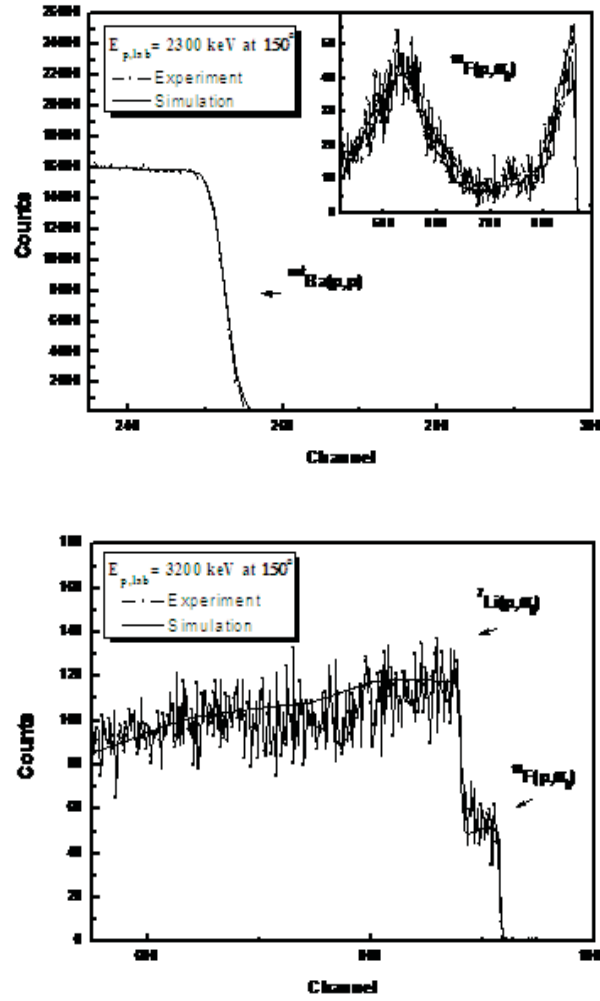


Fig. 3. Experimental spectra taken at 150° whilst irradiating the thick and mirror-polished BaF₂ (a) and LiF (b) targets at 2300 and 3200 keV respectively. In the inset, spectra are presented in the range corresponding to the $^{19}\text{F}(p,\alpha)$ reaction.

again into account a very small energy step for the incoming and outgoing particles, the effect of multiple scattering, the beam ripple, ZBL stopping power data, and Chu and Yang's straggling model as implemented in the SIMNRA code. The Rutherford differential cross sections for the scattered protons from Au and Ba were also used for the simulated spectra. Typical such spectra at 150° at 2300 and 3200 keV are presented in Fig. 3a-b respectively, which show the excellent reproduction of the experimental spectra in the energy range corresponding to the studied $^7\text{Li}(p,\alpha_0)^4\text{He}$ and $^{19}\text{F}(p,\alpha_0)^{16}\text{O}$ reactions, thus validating the obtained cross-section datasets. It is important to note here, that in Fig.3b, the reproduction of the thick LiF target spectrum by the simulated one verifies not only the accuracy of the obtained differential cross sections involved, but also the validity of the Li:F ratio in the thin target, as

determined by the ERDA measurements.

4 Conclusions

A detailed study of differential cross sections of the ${}^7\text{Li}(p,p_0){}^7\text{Li}$, ${}^7\text{Li}(p,\alpha_0){}^4\text{He}$, ${}^7\text{Li}(p,p_1){}^7\text{Li}$, and ${}^{19}\text{F}(p,p_0){}^{19}\text{F}$, ${}^{19}\text{F}(p,\alpha_0){}^{16}\text{O}$, ${}^{19}\text{F}(p,\alpha_{1,2}){}^{16}\text{O}$ reactions for backward detector angles (between 140° and 170° , in steps of 10°) and for the proton energy beam range $E_{p,lab} \sim 1500\text{--}7000$ keV, has been presented. The obtained differential cross-section values have been validated through benchmarking experiments and are already available to the scientific community through the IBANDL nuclear database from IAEA [www-nds.iaea.org/ibandl/].

References

- [1] A. Caciolli, M. Chiari, A. Climent-Font, M.T. Fernandez-Jimenez, G. Garcia-Lopez b, F. Luca-relli, S. Nava, A. Zucchiatti, Nucl. Instr. Meth. B 249 (2006) 95.
- [2] U. Fasoli, D. Toniolo, G. Zago, Nuovo Cimento 34 (1964) 542.
- [3] P.R. Malmberg, Phys.Rev. 101 (1956) 114.
- [4] N. Sarma, K.S. Jayaraman, C.K. Kumar, Nucl. Phys. 44 (1963) 205.
- [5] D. Dieumegard, B. Maurel, G. Amsel, Nucl. Instr. Meth. 168 (1980), 93.
- [6] H. Orihara, M. Baba, M. Akiyama, S. Iwasaki, T. Nakagawa, H. Ueno, M. Watanabe, Journal of the Physical Society of Japan 29 (3), (1970) 533.
- [7] P.D. Forsyth et al., Nucl. Phys. 67, 517-528 (1965).
- [8] I.I. Bondouk, S. Saad, Atomkernenergie 29 (4), (1977) 270.
- [9] A.F. Gurbich, Personal Communication and www-nds.iaea.org/ibandl/.
- [10] M. Mayer, “*SIMNRA, a Simulation Program for the Analysis of NRA, RBS and ERDA*”, Proceedings of the 15th CAARI, J. L. Duggan and I. L. Morgan (eds), AIP Conf. Proc. 475, (1999) 541.
- [11] J.F. Ziegler, J.P. Biersack, U. Littmark, The Stopping and Range of Ions in Solids, Pergamon Press, New York, 1985.
- [12] H.H. Andersen, J.F. Ziegler, Hydrogen Stopping Powers and Ranges in All Elements, in: The Stopping and Ranges of Ions in Matter, vol. 3, Pergamon Press, New York, 1977.